

Asymmetric Blade Disc Turbine for High Aeration Rates

Andrej Bombač

University of Ljubljana, Faculty for Mechanical Engineering, Slovenia

This paper presents some fluid-dynamic characteristics of modified impellers for air dispersion with high flow rates. An asymmetrically folded blade turbine (ABT) was developed as the last in a series of research studies on modified blades of disk impellers, such as twisted blade turbine (TBT) and other blade shape turbines. The analyses of the modified impeller characteristics in a model scale mixing device includes the measurements of: a) the mixing power in liquid stirring and in the air dispersion up to the occurrence of flooding, b) global gas hold up, c) appearance of flooding, and d) the mixing times in liquid stirring. The energy dissipation of the ABT impeller was found to be very small, in the range of hydrodynamic regimes in industrial scale operations with a power number equal to $Po_{ABT} \sim 1.75$. During aeration in water, the ABT impeller has a very small power draw reduction (less than 16 %) at the same stirrer speed (corresponding to $Fr = 0.3$) and is capable of dispersing substantially higher amounts of air (up to 53 %) than the Rushton turbine is, as well as achieving shorter mixing times. While local mixing time expresses only changes with the time at the measuring location, a CFD analysis was included for better insight into inhomogeneity in the liquid. To compare the efficacy of the ABT impeller with other impellers, some results of our previous research are summarized.

Keywords: liquid mixing, air dispersing, gas holdup, ABT impeller, flooding, mixing time

Highlights

- High efficiency of the newly developed asymmetrically folded blade turbine (ABT) during dispersing of air into water by single impeller stirring.
- Low power number of the ABT impeller in water mixing (1.75).
- High pumping capacity by air dispersing at very small power draw reduction (less than 16 %).
- Capable of dispersing much greater amounts of air (up to 53 %) than the Rushton turbine is.
- The shortest mixing time by the same impeller energy dissipation.
- Some CFD analysis results included for better insight into inhomogeneity in the liquid.

0 INTRODUCTION

Air dispersion in tall, slim fermenters is mostly carried out with multistage impellers to provide high air flow intake, which must be supplied in some fermentation processes in the pharmaceutical industry. Such an impeller can be assembled of two equal impellers, such as dual Rushton turbines in parallel, merging, and diverging flow conditions [1], power consumption [2], mixing rate [3] or flow patterns [4]. The higher the ratio between tank height and its diameter H/T , the higher the number of impellers equidistantly placed to ensure as much uniform void fraction distribution as possible [5] to [8]. Nowadays, a combination of axial and radial impellers [7] and [9] predominates. The choice of a proper impeller for the given geometric configuration of the mixing vessel is of prime importance for the optimal achievement in the fermentation process: a fermenter must have a flow field that provides the organisms with air throughout the entire volume of the liquid. Any dead zone can cause an improperly fermented product due to lack of air. A multi-stage impeller with a proper configuration provides the circulation of substances in the fermenter and most evenly distributes the air throughout the

liquid volume [10]. To determine these conditions, it is necessary to know the main characteristics of the individual impeller, such as the mixing power [11] and [12], gas holdup [11], bubble size and distribution [13] and [14], flooding in gas-liquid systems [8], [15] and [16] and in even more complex three-phase systems [17] and [18], mixing time [19] to [21], etc.

Each impeller dispersing air is limited by the maximum amount of air to be dispersed. Further increasing of the air flow rate causes flooding. From the process operation point of view, flooding is an inefficient operation. Usually, the ring sparger is used for the air intake and is placed in-between the bottom and the lowest impeller. From an extensive study [15] of individual impeller-flooding by gassing in a tall mixing vessel with single, dual (Du) and triple (Tr) Rushton turbines, it was determined that the lowest impeller (Du1 and Tr1, see Fig. 1) is prone to be flooded in both configurations even at lower gas flow rates in comparison to gassing with a single impeller in a standard geometric configuration vessel. Due to lesser pumping capacity, a flooded impeller causes an extremely inhomogeneous gas phase distribution and changes the other basic characteristics, so the lowest impeller is of key importance for effective dispersion.

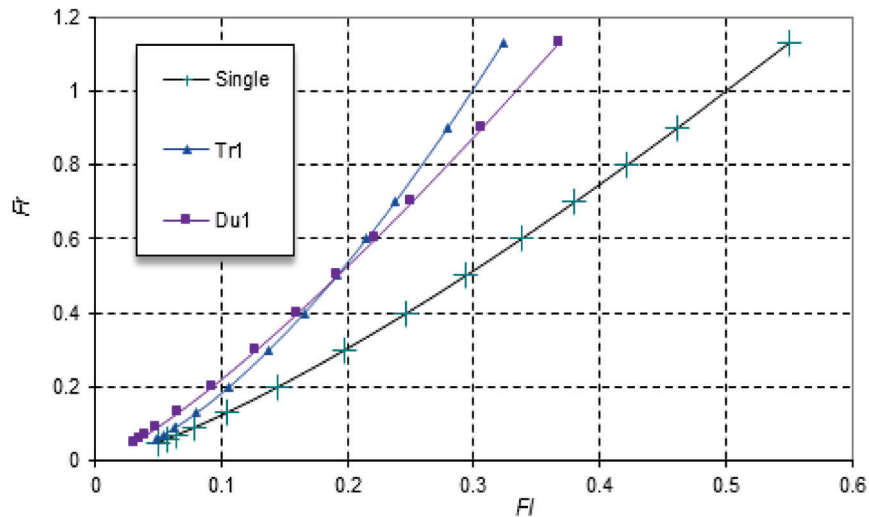


Fig. 1. Individual impeller flooding conditions; comparison of single, the lowest impeller by dual (Du1) and triple-impeller (Tr1) stirring

If an additional enlarged amount of air needs to be dispersed in some fermentation processes [8], at a minimum, the lowest impeller must be replaced with a more capable one in terms of preserving the pumping capacity and the small power reduction as much as possible by gassing. There are many studies in which Rushton turbine modifications [21] and [22] and disk impellers of various blade shapes [19] and [23] to [26] were used to enhance the lowest impeller characteristics.

In the following sections, a modified disk impeller ABT [27] is presented, which is derived from the same basic contour of the standard Rushton turbine (RuT) as well as other modifications; such as split blade disk impeller, twisted blade impeller (TBT) [19] and [28] or double disk impeller [29]. The asymmetrically folded blade turbine (ABT) impeller was developed and patented at the Laboratory for Fluid Dynamics and Thermo-dynamics specifically for dispersing large quantities of air, which (in contrast with the other two developed and gradually improved impellers (the TBT and the split blade turbine) demonstrates air dispersion with the least energy dissipation, a high gas holdup, slight power drawn by aeration, and flooding at much higher gas flow rates than any other impellers. Computational fluid dynamics (CFD) is a very useful tool to analyse transitional phenomenon in space-time domain, which mixing time represents. In that manner, CFD was performed by liquid mixing for the same geometric configuration as the experimental setup. It enabled the visualization of the flow field of different impellers as well as the spreading of poured

hot water, representing the pulse/response technique of measuring the mixing time.

1 EXPERIMENTAL SETUP AND EXPERIMENT

The measurements of the mixing power were carried out in a mixing vessel comprised of an upright cylindrical vessel, made of acrylic glass with an inner diameter $T = 450$ mm with rounded edges and a flat bottom. The mixing drive shaft enabled the placement of up to five impellers of various types and clearances between them in case of multi-stage impeller stirring with a maximum height of the water of 1350 mm. Four baffles of width $T/10$ were axially symmetrically placed perpendicularly to the vessel wall with a gap of 8 mm between the wall and the baffle; the impeller clearance was set to $T/3$. The experimental set-up by single impeller stirring with liquid height $H = T$ is shown in Fig. 2. Impeller speed was measured by IR-pulse transmitter with an absolute error of ± 1 rpm. An HBM transducer enabled torque measurements with an error of ± 0.02 Nm, while the gas flow rate was measured with calibrated rotameters with the error ± 0.4 m³/h, respectively. A more detailed description of the measurement installations and the accuracy of the measured values, the repeatability of the measurements, etc. are given in [15] and [19]. Tap water was used as the working liquid and air from the in-house compressed air, both at room temperature. Mixing time was measured based on pulse-response technique [19] and [30]. One dm³ of hot water at ~ 95 °C was poured into the vessel in cca. 0.5 s just above the location of the thermocouple tip $\{r, z; 65,$

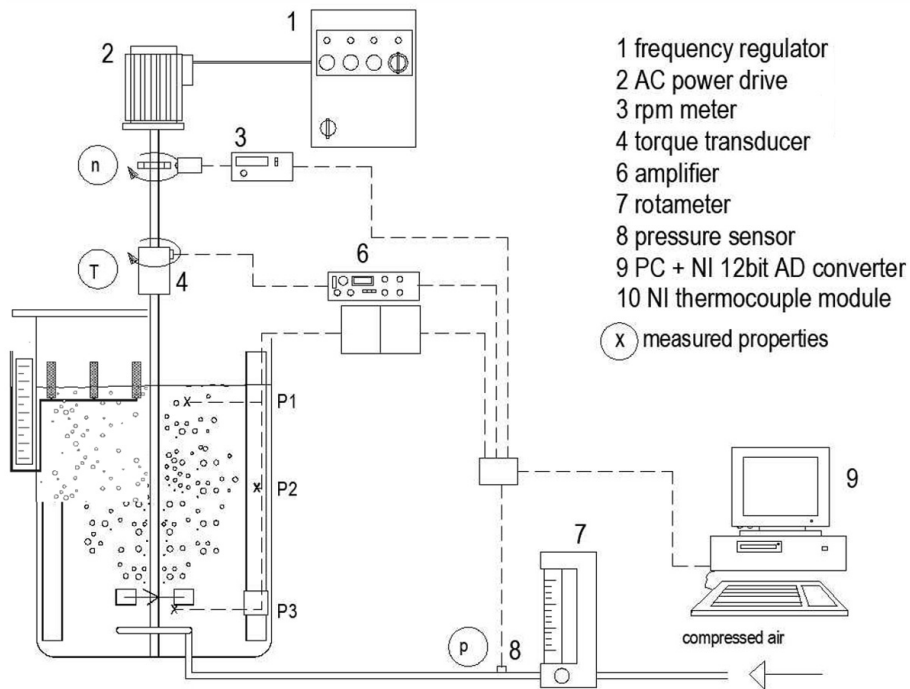


Fig. 2. Experimental set-up

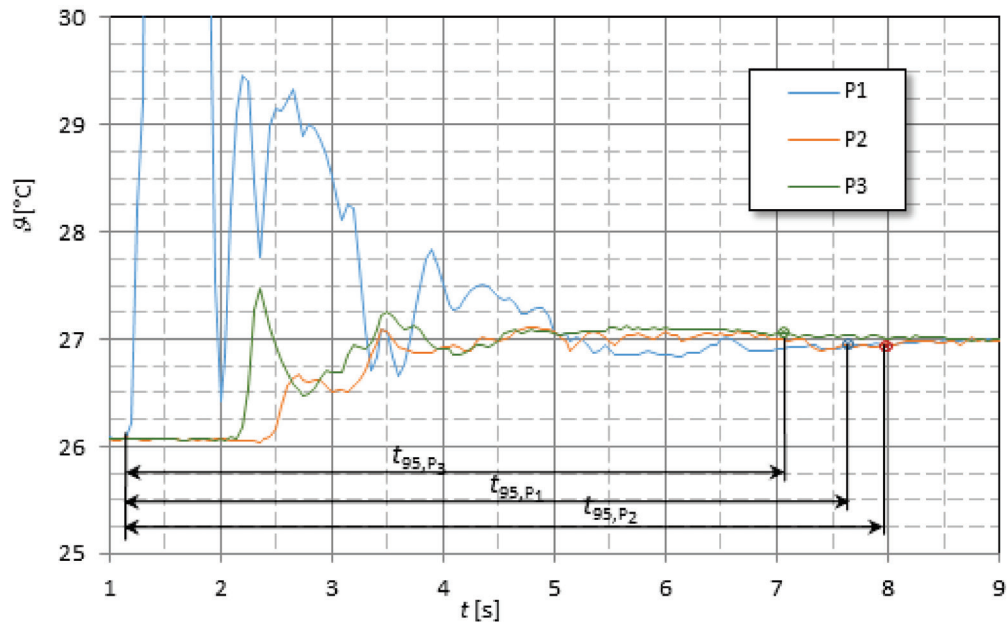


Fig. 3. Mixing times t_{95} based on pulse response at the measurement locations P1, P2, P3

420 mm} to begin the measurements. This location was chosen based on literature data [30] according to which mixing times were measured at three different locations (below the surface, just under the lower edge of the impeller and near the vessel wall) and varied from -10 % to +6 % in comparison with their mean

value. A thin non-insulated thermocouple (Ni-CrNi, type K) of 0.2 mm of diameter tip was used to provide a quick response, which was analysed previously and found to be between 440 °C/s and 550 °C/s. The mixing time t_{95} is defined as the difference between the final time (t_f), when the temperature stabilizes

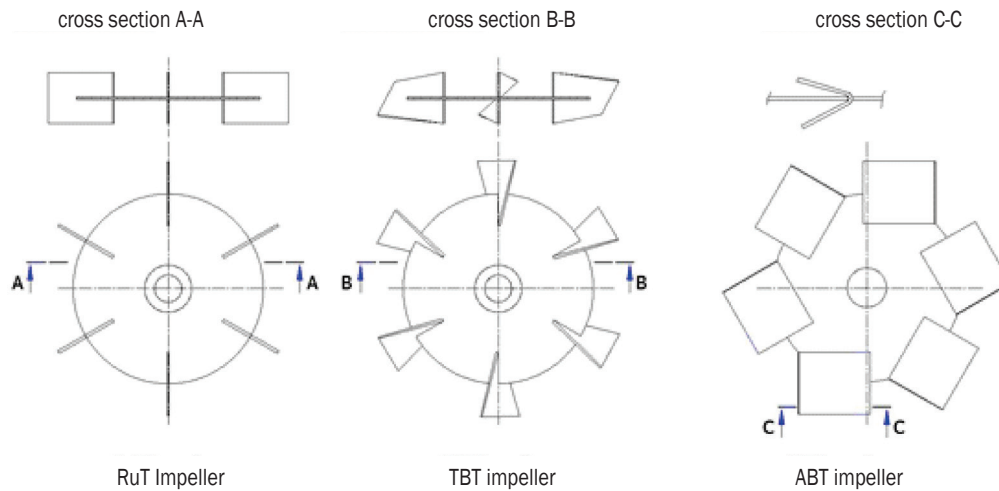


Fig. 4. A Rushton turbine and both modified impellers

within $\pm 5\%$ of the final average temperature, and the start time (t_s) of the pulse entry. The mixing times were calculated from temperatures recorded at three locations defined as: P_1 location (r_1, z_1); ($T/4.7$ from the impeller centre line, $T/4.5$ from the level), P_2 location (r_2, z_2); ($T/2.2$ from the axis of the impeller, $T/3$ from the level) and P_3 location (r_3, z_3); ($T/8$ from the axis of the impeller, $T/50$ from the edge of the impeller) and averaged $(t_{95,P1} + t_{95,P2} + t_{95,P3})/3$. Fig. 3 shows separate temperature responses at the all three locations after the pulse input (poured hot water) by stirring with ABT impeller. The sampling frequency of the measuring temperature was set to 10 Hz; each measurement lasted 60 s.

The global gas holdup measurements were performed with improved three-point “level taker”, which based originally on the change of the liquid level height only in one location and was defined for a cylindrical vessel as:

$$\alpha_g = (H_g - H) / H_g, \quad (1)$$

where H_g means the liquid level under gassing and H is the liquid level by liquid mixing. Each α_g was measured at constant impeller speed with a stepwise increase of the air flow rate. The measurements of the height were taken for each individual hydrodynamic regime five times; their average value was used for further analysis. All the impellers used (RuT, TBT, and ABT) are shown in Fig. 4. The blade of the ABT impeller is in the middle by width (w) folded in the form of the letter “V” and placed so that the upper part has a smaller slope than the lower part does, while the upper part is longer than the lower part, as shown in Fig. 4, cross section C-C.

All impellers (RuT, TBT, and ABT) have the same disk diameter, the same width (b) and height (w) of the blades and the impeller diameter ($T/3$), as shown in Fig. 4.

2 RESULTS AND DISCUSSION

A number of measurements were taken in order to determine the basic impeller characteristics for each type of impeller in liquid mixing and in the dispersing of air into water by a standard geometric configuration of the mixing vessel.

2.1 Mixing Power in Water

The mixing power of each individual impeller was measured for various rotational speeds and is expressed with power number $Po = P/(\rho \cdot n^3 \cdot D^5)$, while the impeller rotational speed is expressed with the Reynolds number $Re = D^2 \cdot n/\nu$.

The rotational impeller speed increased from 50 rpm to 650 rpm. As shown in Fig. 5, in the range $Re > 110,000$, the Po value for the ABT impeller stabilizes with an averaged value of $Po \sim 1.75$, while the average value for the standard RuT impeller when stabilized and without surface aeration is ~ 5.13 . At $Re > 150,000$, the power number of the RuT impeller decreases due to surface aeration, i.e. air being sucked from the surface in the liquid. Such a hydrodynamic regime is treated as an air dispersion with a low gas holdup. In mixing with the TBT and ABT impeller, no surface aeration in the same range of impeller speeds was detected. Therefore, why the ABT power curve stabilizes at a higher Re number can be attributed

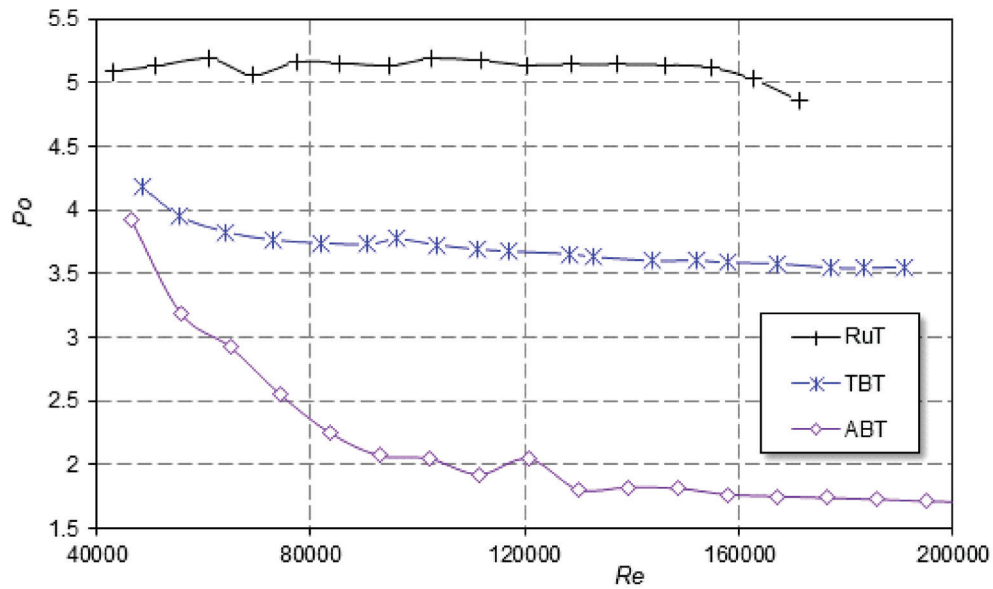


Fig. 5. Power number of various disk impellers by mixing in water

to its hollow blade shape; these types of impellers develop fully turbulent regime in the baffled tank at higher impeller speeds [23].

2.2 Dispersion of Air in Water

The mixing power in air dispersion is usually found to be lesser than mixing in a liquid and decreases with an increase of air flow rate. This is due to the weaker pumping capacity of the impeller, since the negative

pressure region behind the blades is filled with air, i.e. so-called gas-filled cavities. With an increase in air flow, the gas cavities become greater, while the pumping capacity of the impeller becomes ever weaker. Flooding occurs when the buoyancy forces of the gas phase dominate the weak primary circulation of the impeller discharge flow. During the measurement of the mixing power, this state can be reflected as a local increase in power (with regard to the previous regime), and the corresponding relationship is marked

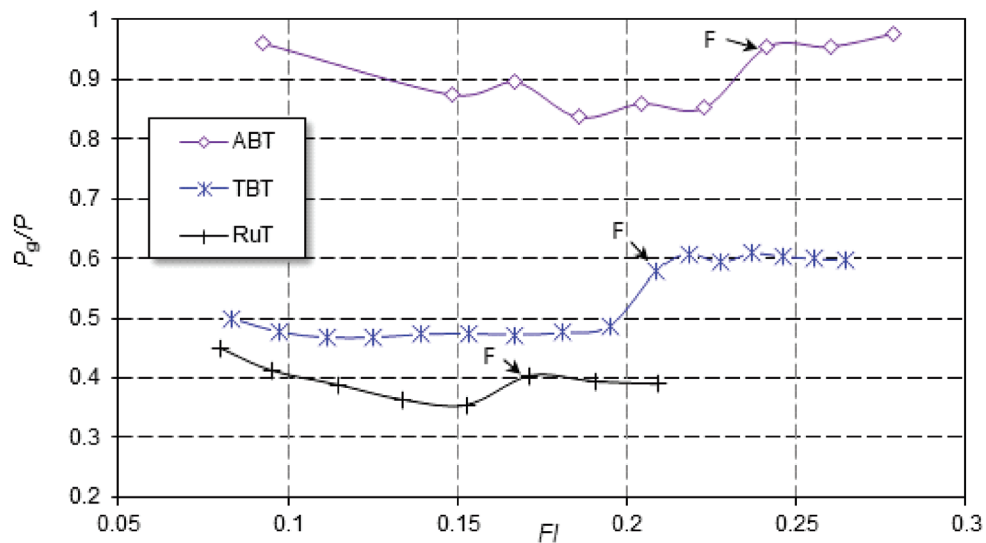


Fig. 6. Power drawn under gassing at Fr = 0.3

as flooding $(P_g/P)_F$ while the condition just before flooding as loading $(P_g/P)_L$, respectively, and the transition itself is the loading-to-flooding transition [16]. In Fig. 6, the ratio P_g/P is shown in air dispersion with the studied impellers in dependence on the flow number $Fl = q/(n \cdot D^3)$ at constant impeller speed expressed with Froude number $Fr = n^2 \cdot D/g$. It is obvious that the RuT impeller floods first at $Fl \sim 0.17$ while the primary circulation of the impeller discharge flow weakens with increasing gas flow rate, and the mixing power dissipation decreases by 65 %.

With a modified twisted-blade shape, the TBT impeller floods at a somewhat higher flow number

$Fl \sim 0.21$, but during dispersion, there is still a 52 % decrease in power. Real improvement of gas dispersion can be seen only with the ABT impeller, which floods at $Fl = 0.24$ and shows a very small power draw under gassing: only 18 %. That means that the ABT impeller still maintains the circulation of dispersed air in the vessel even with quite higher air flow rates. Another flooding recognition method in single-impeller dispersion [16] used in our study of ABT impeller is based on the global gas holdup drop, as shown in Fig. 7. With an increase of air inflow into the liquid, the gas holdup rises to a stagnation point and soon, with a further minimal increase in the air intake, flooding

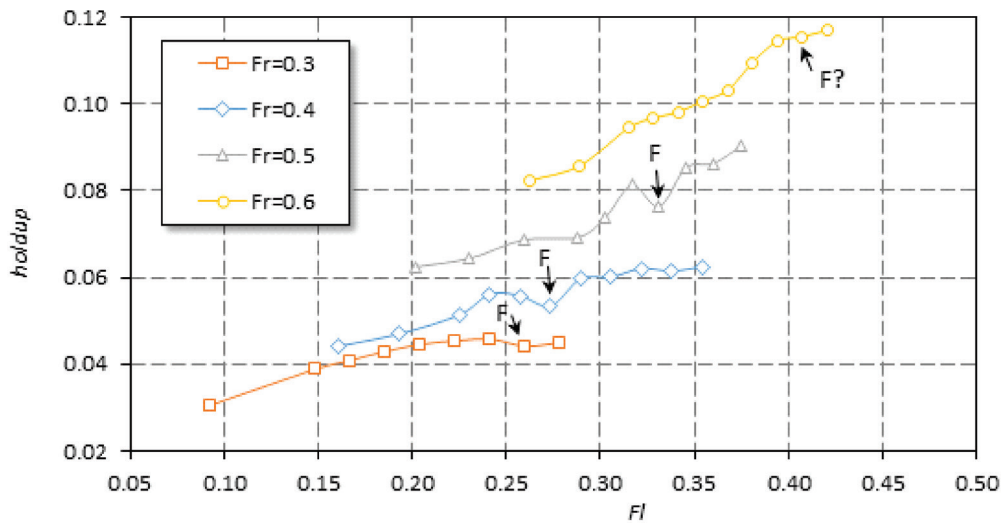


Fig. 7. Global gas holdup of the ABT impeller depending on the flow number Fl

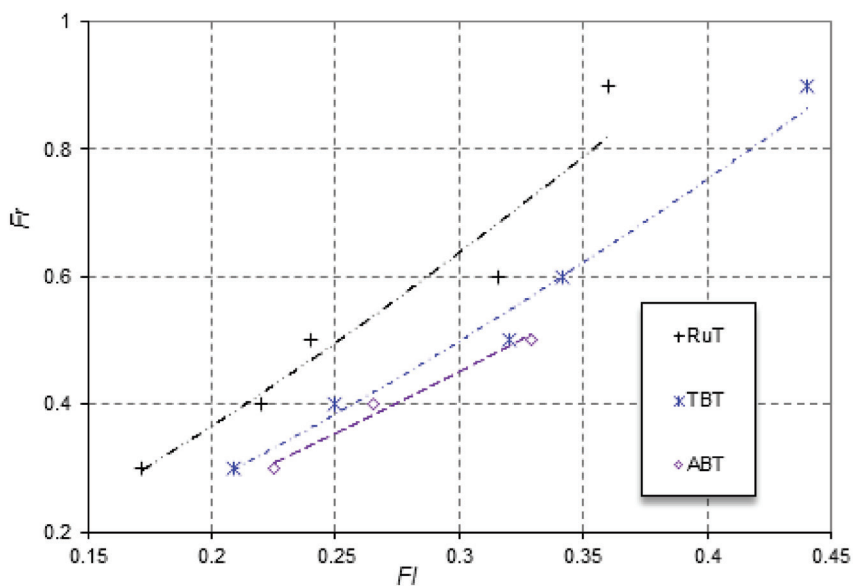


Fig. 8. Measured LFT for the studied impellers: curves correlated according to Eq. (2)

occurs (F). In Fig. 7, flooding conditions are shown as a local decrease in the global gas holdup and are evident at $Fr = 0.3$, $Fr = 0.4$ and $Fr = 0.5$, while at $Fr = 0.6$ no flooding was able to be detected.

Thus, on the basis of the measurement results of the studied impellers, the influence of the different disk impellers on the flooding transition can be seen in the flow map in Fig. 8. Curves represent loading to flooding transition (LFT) correlation criteria

$$Fr = k_1 \cdot Fl^{k_2}, \quad (2)$$

with the coefficients k_1 and k_2 and the correlation coefficient R shown in Table 1.

Table 1. Parameters of the regression curve by Eqs. (1) and (2)

Impeller/coef.	ABT	TBT	RuT
k_1	1.912	2.786	3.340
k_2	1.216	1.429	1.375
k_3	32.64	19.913	32.978
k_4	-0.464	-0.3162	-0.378
R_{LFT}	0.991	0.991	0.976
R_{t95}	0.970	0.960	0.923

The ABT impeller is clearly capable of dispersing an even somewhat greater amount of air than the TBT impeller prior to flooding by higher impeller rotational speeds (Fr). However, the basic difference between their functioning is in the power drawn which is significantly lesser with the ABT.

2.3 Mixing Time during Liquid Mixing

The mixing times of the studied impellers were approximated according to the criteria [19] depending on the impeller power:

$$t_{95} = k_3 \cdot P^{k_4}, \quad (3)$$

where the coefficients k_3 and k_4 and the correlation coefficient R are shown in Table 1.

In general, it is clearly seen that with a greater mixing power the mixing time for all given impellers is shorter, as can be seen in Fig. 9. The greater mixing power essentially represents the greater pumping capacity of the impeller and, consequently, more intensive circulation which is reflected in a shorter mixing time. The difference in the mixing time among studied disk impellers of equal *side view contour* are at the same mixing power related only to the form of the blades of individual impellers, which form and direct the impeller discharge flow. For example, it is clear that the RuT impeller mixing times are very long, even twice the times for the ABT impeller,

which, of course, strongly influences the efficiency of the impeller, as will be discussed later.

The measured mixing times were compared with the results of the most cited criterion [7], [20] and [31], which was based on summarized experimental data of mixing times (t_{95}) of different impeller types:

$$t_m = 5.2 \left(\frac{1}{n}\right) \left(\frac{1}{Po^{0.33}}\right) \left(\frac{T}{D}\right)^2. \quad (4)$$

According to Eq. (4), the mixing times are regarded to any impeller type in single impeller mixing by the conditions $1/3 < D/T < 1/2$ and $H = T$. A comparison of the measured values calculated using Eq. 4 shows a relatively good match with the interdependent parameters $P-t_m$, which raises the question of the meaningfulness of comparing absolute values. As can be seen from Fig. 9, the studied TBT and ABT impellers have achieved quite different mixing times by the same mixing power. Specifically, the Power number for the RuT impeller in the standard geometric configuration, according to the literature survey, is found to be between $4.8 \leq Po \leq 6.3$, which differs from our measured value with a relative discrepancy from -7% to 23% . Similarly, various experimental methods of determining the mixing time also differ not only on a physical basis (temperature response, pH change, change in conductivity, discoloration, etc.), but also according to the various criteria for achieving the mixing rate. Thus, the mixing rate can be reached by determination: i) $A_\infty = \pm 0.05 \cdot \Delta A$ [21] and [26] or ii) $A'_\infty = \pm 1\%$ [11], $\pm 5\%$ [32] and [33] or even $\pm 10\%$ [34] where A represents any measured property and A' its fluctuation [29]. If we proceed from the local measurements, then we have to additionally take into account the influence of the location itself (r ; z , ϕ), since the deviations between mixing times were found to be from -6% to 11% of the mean mixing time [11]. In general, the pulse/response method determines the minimal amount of input substance that represents a pulse. In our case, this means 1 dm^3 of hot water (as a pulse) while the pouring of water into the vessel itself takes between 0.5 s and 0.75 s and is directly included in the mixing time, while the injection times of chemicals of much smaller quantities using methods based on conductivity or pH change (injection of 3 ml of acid or salt solution, etc.), or discoloration, are considerably shorter.

The mixing time, expressed with local changes in any arbitrary property, represents only the time that a lack of homogeneity is present at a given location in the vessel, so the mixing time is only a somewhat rough evaluation of mixing quality. Therefore, for a

high-quality product from the process, any difference in homogeneity of the liquid volume is of vital importance, see Fig. 13.

To analyse the mixing efficiency of an individual impeller, direct energy consumption (E - dissipated energy) can be used as a suitable estimate:

$$E = t_{95} \cdot P. \quad (5)$$

Now it is clearly seen (Fig. 10) that the mixing times of the impellers are quite different by the same dissipated energy. For the same mixing time as the ABT impeller (e.g. at 5 s), the TBT impeller dissipates approximately ~ 2.7 times more energy and the RuT ~ 5.2 times more. Due to all the above-mentioned preferences, i.e. a very small reduction of P_g/P under gassing, and simultaneously maintaining

the circulation of a dispersed air in the vessel with quite higher air flow rates, as well as low power consumption, the ABT impeller is very suitable to be placed as the lowest impeller in the case of a multi-stage impeller for dispersing a large gas intakes into the liquid.

A commercial CFD code ANSYS Fluent 14.5 was performed by liquid mixing in a standard geometric configuration tank of equal size as the experimental device to analyse some mixing characteristics of different impeller types. The computational mesh consisted of two parts: the first one represented the stationary part (i.e. the mixing vessel with baffles of 959,040 cells), and the second one represented the rotational part formed from 86,100 cells for the RuT impeller and 327,531 cells for the ABT impeller.

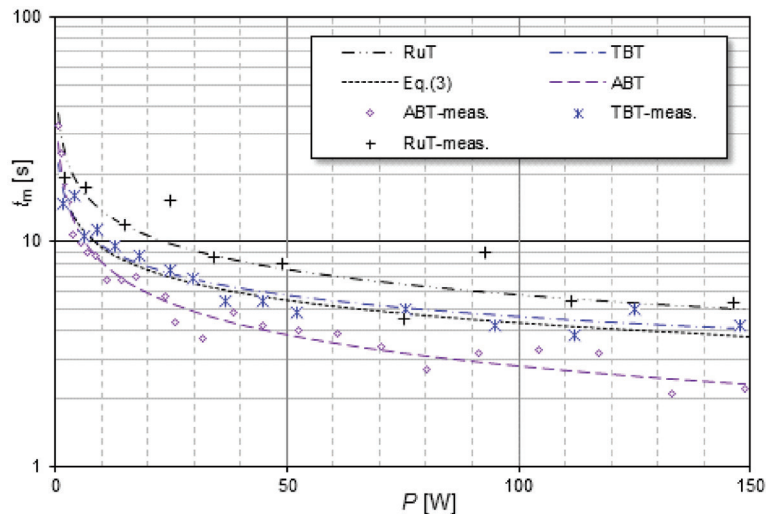


Fig. 9. Mixing time dependence on the mixing power for various disk impellers

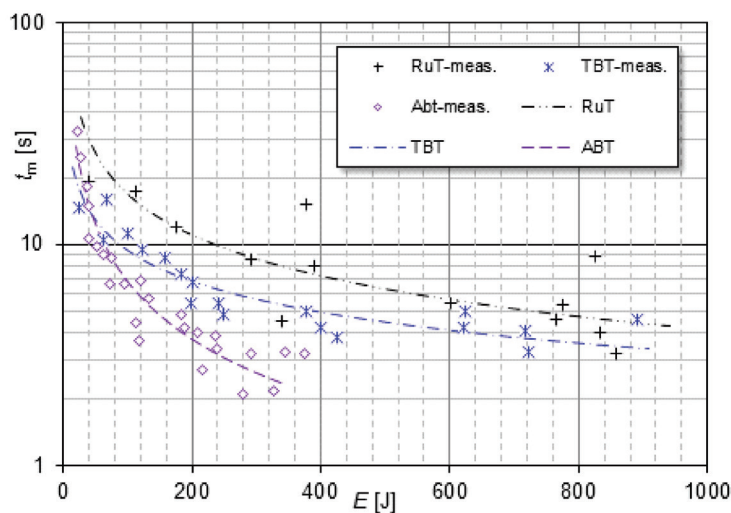


Fig. 10. Mixing time dependence on dissipated energy of various disk impellers

Some characteristics of the approach with *Sliding mesh* and *Reynolds stress model* for turbulence given by an impeller rotational speed of 267 rpm calculated flow field are shown in the following figures. It can be seen that, for example, how the liquid flow field and turbulent kinetic energy differ from one another during the mixing with the Rut, TBT, or ABT impeller. Turbulent kinetic energy by mixing with the RuT impeller with its discharge flow causes the greatest turbulence, as seen in the vertical *r-z* cross-section and in a cross-section at the height of the impeller disk (upper right in Fig. 11). The radially directed discharge flow from the impeller splits at the vessel wall into upper and lower circulation loops, as shown in the flow field with speed vectors shown in Fig. 12. Quite different conditions are seen with the

TBT impeller; it achieved a somewhat lower turbulent kinetic energy, impeller discharge flow during mixing in water is directed axially down-wards (which completely changes with air dispersion and becomes radial) and there is one large circulation loop. The flow pattern in liquid mixing is very similar, otherwise, to the axial impellers whose main purpose is to provide an intensive circulation with the least turbulence. With the ABT impeller, the turbulent kinetic energy is much smaller and is present in a narrower area. The impeller discharge flow is radial and at the wall splits into an upper and lower circulation loop; both circulations are more intense than with the RuT impeller. The CFD calculated power number was $Po_{ABT} = 1.7$, which was $\sim 3.5\%$ higher than the measured one. By stirring with RuT impeller, the CFD-calculated power

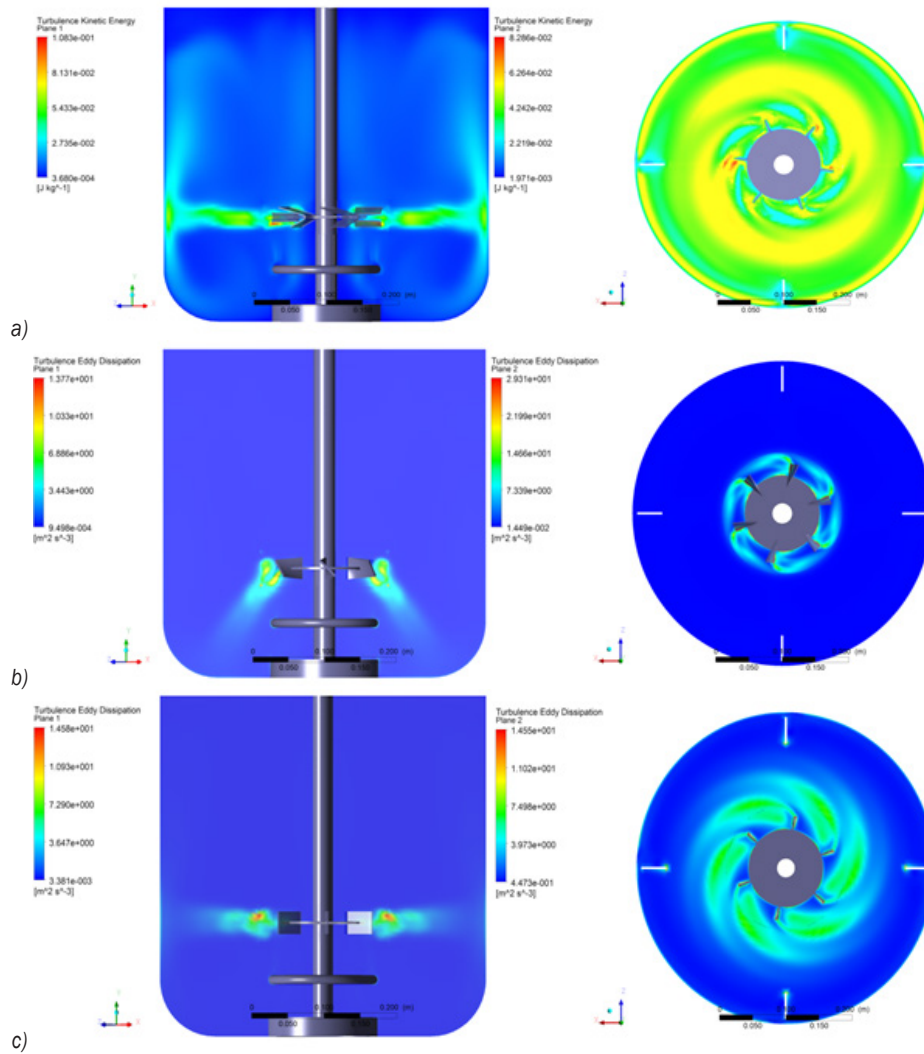


Fig. 11. Turbulence kinetic energy by mixing with a) RuT, b) TBT, and c) ABT impellers [28]

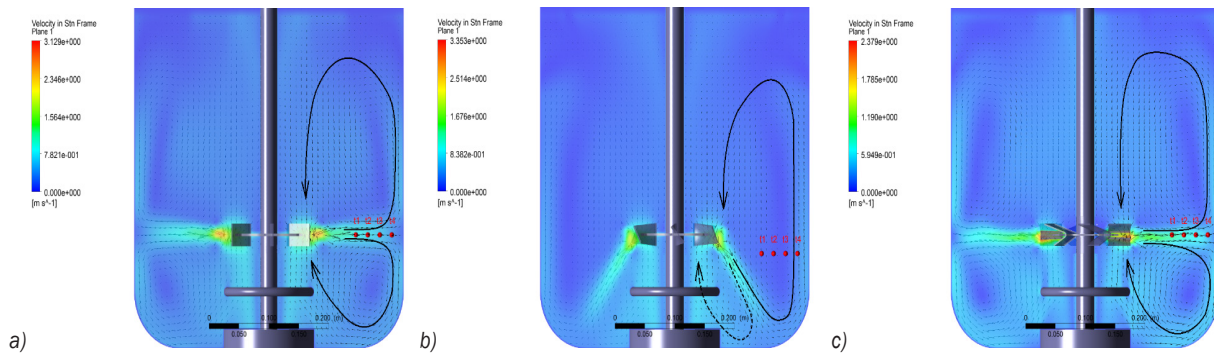


Fig. 12. Flow field; velocity vectors for a) RuT, b) TBT, and c) ABT impellers [28]

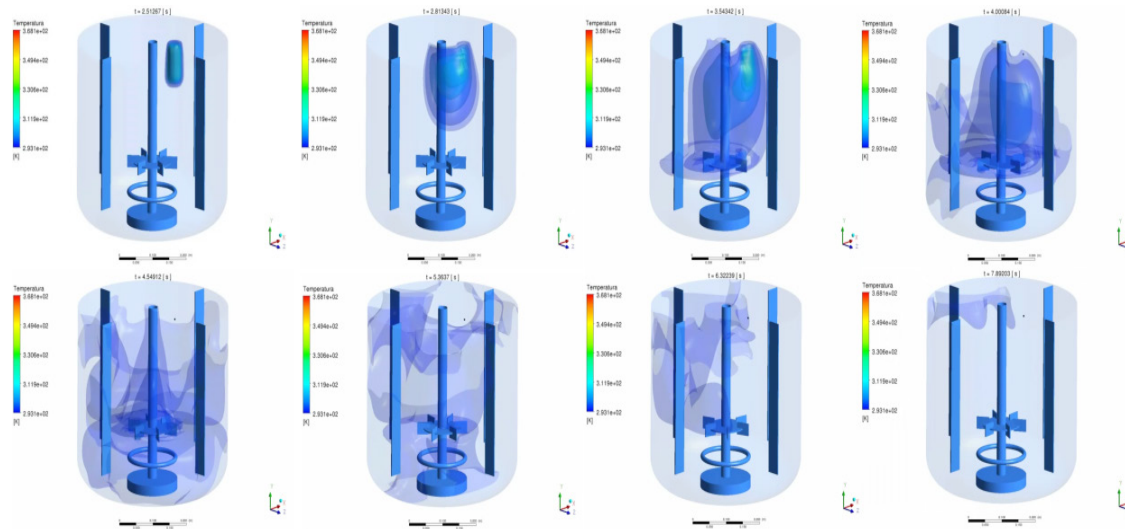


Fig. 13. Spreading of hot water (pulse) in the flow field using the RuT impeller after 2.5 s, 2.8 s, 3.1 s, 4.0 s, 4.5 s, 5.3 s, 6.2 s, and 7.8 s [33]

number was $Po_{RuT} = 4.0$ representing a 22 % lower value than the measured one, and by TBT impeller $Po_{TBT} = 2.49$ representing a 33 % lower value than the measured one, respectively [28]. CFD is a very useful tool to analyse a transitional phenomenon in space-time domain; which is what mixing time represents. The simulation was performed with 1 dm³ of hot water at the P1 location in the same manner as in the experiment. The spreading of the added hot water (pulse) in the r - z cross-section plane is shown in Fig. 13. Spreading started in the already developed flow field of water mixing with the RuT impeller by $Fr = 0.3$. The blue colour represents the state of mixing, greater than ± 5 % of the final value. Looking at the mixing-over-time domain, the mixing time (expressed as the local change in any arbitrary property) represents only the time when a lack of homogeneity is present at a given location in the vessel, which confirms our assumption. This is particularly clearly

seen at 6.2 s and 7.8 s, when the proposed mixing rate has already reached the marked location P1 despite the presence of inhomogeneity in the liquid in its immediate vicinity. According to measured mixing time, by the same impeller speed, which was equal to 8.5, the CFD-calculated mixing time was in good agreement.

3 CONCLUSIONS

This article presents the efficiency of the asymmetrically folded blade turbine (ABT) during the mixing and dispersing of air into water with a single impeller in the standard geometric configuration of the mixing vessel. To compare the efficiency of this impeller, this paper also summarizes some findings of our previous research on other disk impellers (RuT, TBT, and split blade disk turbine). The mixing power measurements were performed in liquid and in

the dispersion of air into liquid by a single impeller stirring up to the eventual flooding appearance (LFT).

The power number of the ABT impeller in water mixing is low, and it's almost constant value equals $Po \sim 1.75$.

In the dispersion of air into water, the ABT impeller maintains its pumping capacity, which arises from the small power draw (less than 16 %) with the capability of dispersing much greater amounts of air (up to 53 %) than a Rushton turbine or TBT impeller.

Of all the impellers presented here, the mixing times are shortest for the ABT impellers at the same impeller power. Even more noticeable is the difference in the impeller efficiency, such that at the same mixing time of 5 s with the ABT impeller the TBT impeller dissipates approximately 3 times and the RuT impeller even 5.5 times more energy than the ABT impeller does.

Analyses of some mixing characteristics, such as liquid circulation, impeller power dissipation, mixing time and others, were also carried out using a CFD approach for specific purposes with the above-mentioned impellers. In this manner, the visualization of the flow field and other fluid dynamic characteristics can be seen very clearly; for example, spreading of hot water for a better understanding of mixing time characteristics.

4 ACKNOWLEDGEMENTS

The author would like to thank the Slovenian Ministry of Science for financial support under the current program No. P2-0162.

5 NOMENCLATURES

A arbitrary property,
 A' property fluctuation,
 b blade width, [m]
 D impeller diameter, [m]
 E impeller energy dissipation, [J]
 Fl flow number, [-]
 Fr froude number, [-]
 g gravitational acceleration [ms^{-2}]
 H liquid height in the vessel, [m]
 H_g liquid height by gassing, [m]
 k_1, k_2, k_3, k_4 coefficients, [-]
 q gas volume flow rate, [m^3s^{-1}]
 n rotational impeller speed, [s^{-1}]
 P impeller power by liquid mixing, [W]
 Po power number, [-]
 P_g gassing power, [W]
 R correlation coefficient, [-]

Re Reynolds number, [-]
 t_{95} mixing time, [s]
 T vessel diameter, [m]
 t_s start time, [s]
 t_f final time, [s]
 t_m mixing time, [s]
 r, z coordinates of r-z plane, [m]
 w blade height, [m]
 ν kinematic viscosity, [m^2s^{-1}]
 α_g gas holdup, [%]
 ρ density, [kgm^{-3}]
 ϑ temperature, [$^{\circ}\text{C}$]

6 REFERENCES

- [1] Khopkar, A.R., Tanguy, P.A. (2008). CFD simulation of gas-liquid flows in stirred vessel equipped with dual Rushton turbines: influence of parallel, merging and diverging flow configurations. *Chemical Engineering Science*, vol. 63, no. 14, p. 3810-3820, DOI:10.1016/j.ces.2008.04.039.
- [2] Taghavi, M., Zadhaffari, R., Moghaddas, J., Moghaddas, Y. (2011). Experimental and CFD investigation of power consumption in a dual Rushton turbine stirred tank. *Chemical Engineering Research and Design*, vol. 89, no. 3, p. 280-290, DOI:10.1016/j.cherd.2010.07.006.
- [3] Zadhaffari, R., Moghaddas, J.S., Revstedt, J. (2009). A mixing study in a double-Rushton stirred tank. *Computers & Chemical Engineering*, vol. 33, no. 7, p. 1240-1246, DOI:10.1016/j.compchemeng.2009.01.017.
- [4] Devi, T.T., Kumar, B. (2013). Comparison of flow patterns of dual Rushton and CD-6 impellers. *Theoretical Foundations of Chemical Engineering*, vol. 47, no. 4, p. 344-355, DOI:10.1134/S0040579513040210.
- [5] Zhang, L., Pan, Q., Rempel, G.L. (2006). Liquid phase mixing and gas hold-up in a multistage-agitated contactor with co-current upflow of air/viscous fluids. *Chemical Engineering Science*, vol. 61, no. 18, p. 6189-6198, DOI:10.1016/j.ces.2006.06.001.
- [6] Xie, M., Xia, J., Zhou, Z., Zhou, G., Chu, J., Zhuang, Y., Zhang, S., Noorman, H. (2014). Power consumption, local and average volumetric mass transfer coefficient in multiple-impeller stirred bioreactors for xanthan gum solutions. *Chemical Engineering Science*, vol. 106, p. 144-156, DOI:10.1016/j.ces.2013.10.032.
- [7] Magelli, F., Montante, G., Pinelli, D., Paglianti, A. (2013). Mixing time in high aspect ratio vessels stirred with multiple impellers. *Chemical Engineering Science*, vol. 101, p. 712-720, DOI:10.1016/j.ces.2013.07.022.
- [8] Bombač, A. (2013). *Loading-Flooding Transition and Local Void Fraction Measurements on Industrial Fermentor 30 m3. Report*. University of Ljubljana, Faculty of Mechanical Engineering, Ljubljana. (in Slovene)
- [9] Bombač, A., Senica, D., Žun, I. (2012). Flooding detection measurements on the pilot fermentor. *Conference Proceedings Kuhljevi dnevi*, p. 1-8. (in Slovene)
- [10] Tang, W., Pan, A., Lu, H., Xia, J., Zhuang, Y., Zhang, S., Chu, J., Noorman, H. (2015). Improvement of glucoamylase

- production using axial impellers with low power consumption and homogeneous mass transfer. *Biochemical Engineering Journal*, vol. 99, p. 167-176, DOI:10.1016/j.bej.2015.03.025.
- [11] Haucine, I., Plasari, E., David, R. (2000). Effects of the stirred tank's design on power consumption and mixing time in liquid phase. *Chemical Engineering & Technology*, vol. 23, no. 7, p. 7-15, DOI:10.1002/1521-4125(200007)23:7<605::AID-CEAT605>3.0.CO;2-0.
- [12] Ochieng, A., Onyango, M.S. (2008) Homogenization energy in a stirred tank. *Chemical Engineering and Processing: Process Intensification*, vol. 47, no. 9-10, p. 1853-1860, DOI:10.1016/j.cep.2007.10.014.
- [13] Barigou, M., Greaves, M. (1992). Bubble-size distributions in a mechanically agitated gas-liquid contactor. *Chemical Engineering Science*, vol. 47, no. 8, p. 2009-2025, DOI:10.1016/0009-2509(92)80318-7.
- [14] Bao, Y., Chen, L., Gao, Z., Chen, J., (2010). Local void fraction and bubble size distributions in cold-gassed and hot-sparged stirred reactors. *Chemical Engineering Science*, vol. 65, no. 2, p. 976-984, DOI:10.1016/j.ces.2009.09.051.
- [15] Bombač, A., Žun, I. (2006). Individual impeller flooding in aerated vessel stirred by multiple-Rushton impellers. *Chemical Engineering Journal*, vol. 116, no. 2, p. 85-95, DOI:10.1016/j.cej.2005.10.009.
- [16] Bombač, A., Žun, I. (2002). Flooding-recognition methods in a turbine-stirred vessel. *Strojniški vestnik - Journal of Mechanical Engineering*, vol. 48, no. 12, p. 663-676.
- [17] Cai Q., Dai, G. (2010). Flooding characteristics of hydrofoil impeller in a two- and three-phase stirred tank. *Chinese Journal of Chemical Engineering*, vol. 18, no. 3, p. 355-361, DOI:10.1016/S1004-9541(10)60231-5.
- [18] Cheng, D., Wang, S., Yang, C., Mao, Z. (2017). Numerical simulation of turbulent flow and mixing in gas-liquid-liquid stirred tanks. *Industrial & Engineering Chemistry Research*, vol. 56, no. 45, p. 13050-13063, DOI:10.1021/acs.iecr.7b01327.
- [19] Bombač, A., Žun, I. (2006). Power consumption and mixing time in stirring with modified impellers. *Proceedings of the 12th European Conference on Mixing*, p. 153-160, DOI:10.13140/2.1.2673.2809.
- [20] Ascanio, G. (2015). Mixing time in stirred vessels: A review of experimental techniques. *Chinese Journal of Chemical Engineering*, vol. 23, no. 7, p. 1065-1076, DOI:10.1016/j.cjche.2014.10.022.
- [21] Nienow, A.W. (1997). On impeller circulation and mixing effectiveness in the turbulent flow regime. *Chemical Engineering Science*, vol. 52, no. 15, p. 2557-2565, DOI:10.1016/S0009-2509(97)00072-9.
- [22] Su, T., Yang, F., Li, M., Wu, K. (2018). Characterization on the Hydrodynamics of a Covering-plate Rushton Impeller. *Chinese Journal of Chemical Engineering*, in press, DOI:10.1016/j.cjche.2017.11.015.
- [23] Ghotli, R.A., Abdul Aziz, A.R., Shaliza I., Baroutian, S., Arami-Niya, A. (2013). Study of various curved-blade impeller geometries on power consumption in stirred vessel using response surface methodology. *Journal of the Taiwan Institute of Chemical Engineers*, vol. 44, no. 2, p. 192-201, DOI:10.1016/j.jtice.2012.10.010.
- [24] Cooke, M., Heggs, P.J. (2005). Advantages of the hollow (concave) turbine for multi-phase agitation under intense operating conditions. *Chemical Engineering Science*, vol. 60, no. 20, p. 5529-5543, DOI:10.1016/j.ces.2005.05.018.
- [25] Ameer, H., Bouzit, M. (2012). Mixing in shear thinning fluids. *Brazilian Journal of Chemical Engineering*, vol. 29, no. 2, p. 349-358, DOI:10.1590/S0104-66322012000200015.
- [26] Vasconcelos, J.M.T., Orvalho, S.C.P., Rodrigues, A.M.A.F., Alves, S.S. (2000). Effect of blade shape on the performance of six bladed disk turbine impellers. *Industrial & Engineering Chemistry Research*, vol. 39, no. 1, p. 203-213, DOI:10.1021/ie9904145.
- [27] Bombač, A. (2013). *Disc Mixer with Asymmetrical Bended Blades: Patent SI 24012 (A)*. The Slovenian Intellectual Property Office, Ljubljana.
- [28] Matijević, I. (2013). *Numerical Simulation of Mixing in the Agitated Vessel with Different Impellers*. Diploma work, University of Ljubljana, Faculty of Mechanical Engineering, Ljubljana.
- [29] Bombač, A., Beader, D., Žun, I. (2012). Mixing times in a stirred vessel with a modified turbine. *Acta Chimica Slovenica*, vol. 59, no. 4, p. 707-721.
- [30] Paul, L.E., Atiemo-Obeng A.V., Kresta M.S. (eds.) (2004). *Handbook of Industrial Mixing – Science and Practice*. John Wiley & Sons, Hoboken.
- [31] Rodgers, T.L., Gangolf, L., Vannier, C., Parriaud, M., Cooke, M. (2011). Mixing times for process vessels with aspect ratios greater than one. *Chemical Engineering Science*, vol. 66, no. 13, p. 2935-2944, DOI:10.1016/j.ces.2011.03.036.
- [32] Woziwodzki, S., Broniarz-Press, L., Ochowiak, M. (2010). Effect of eccentricity on transitional mixing in vessel equipped with turbine impellers. *Chemical Engineering Research and Design*, vol. 88, no. 12, p. 1607-1614, DOI:10.1016/j.cherd.2010.04.007.
- [33] Matijević, I., Bombač, A., Mencinger, J., Žun, I. (2013). The comparison of calculated mixing time for two impellers with two computing methods. *Conference Proceedings Kuhljevi dnevi*, p. 113-120. (in Slovene)
- [34] Bujalski, J.M., Javorski, Z., Bujalski, W., Nienow, A.W. (2002). The influence of the addition position of a tracer on CFD simulated mixing times in a vessel agitated by a Rushton turbine. *Chemical Engineering Research and Design*, vol. 80, no. 8, p. 824-831, DOI:10.1205/026387602321143354.